Materials Science and Engineering B xxx (2015) xxx–xxx

Contents lists available at ScienceDirect

Materials Science and Engineering B

journal homepage: www.elsevier.com/locate/mseb

Layer-by-Layer films based on biopolymers extracted from red seaweeds and polyaniline for applications in electrochemical sensors of chromium VI

Emanuel Airton de Oliveira Farias[a], Marianne Corrêa dos Santos[a], Natália de Araujo Dionísio[a], Patrick V. Quelemes[a], José Roberto de Sousa Almeida Leite[a], Peter Eaton[c], Durcilene Alves da Silva[a], Carla Eiras[a,b,*]

[a] *Núcleo de Pesquisa em Biodiversidade e Biotecnologia, BIOTEC, CMRV, UFPI, Parnaíba, PI 64202-020, Brazil*
[b] *Laboratório Interdisciplinar de Materiais Avançados, LIMAV, CCN, UFPI, Teresina, PI 64049-550, Brazil*
[c] *REQUIMTE, Faculdade de Ciências da Universidade do Porto, Rua do Campo Alegre, Porto 4169-007, Portugal*

ARTICLE INFO

Article history:
Received 18 February 2015
Received in revised form 23 April 2015
Accepted 20 May 2015
Available online xxx

Keywords:
Polyaniline
Algae polysaccharides
Electrochemical stability
Thin films
Chromium VI detection

ABSTRACT

This paper proposes a new application for natural polysaccharides (agar and carrageenan), both extracted from the cell wall of red seaweeds. Thin films were prepared by the Layer-by-Layer (LbL) self-assembly technique onto ITO (tin-doped indium oxide), where the polysaccharides of interest were deposited in layers alternating with polyaniline (PANI). The films developed were characterized by cyclic voltammetry (CV), ultraviolet–visible spectroscopy (UV–vis) and atomic force microscopy (AFM). Results showed the presence of agar as well as carrageenan, which improves the electrochemical stability of the conducting polymer in an acid medium. The interactions at the molecular level between PANI and the biopolymers affected the most appropriate sequence of deposition as employed in the process of material immobilization and also influenced the resulting morphology. Among the films studied, the most promising system as regards electrochemical measurements was the ITO/agar/PANI system, which was subsequently employed in the electrochemical detection of chromium (VI).

1. Introduction

The science and technology of thin films has an essential role in high-technology industries, due to the versatility of applications in which these materials may be used [1]. For this reason, thin films have been extensively studied, particularly as regards their nanostructures, properties, and forms of preparation [2].

Amongst the preparation methods for thin films of soft materials, the Layer-by-Layer (LbL) self-assembly technique has received recent attention partly due to its experimental simplicity, and because it enables studies of molecular interactions between a wide variety of materials [3,4]. In addition, when working with materials in the form of thin films, rather than as powder or solution, it is possible to obtain highly organized structures at the molecular level and controlling the thickness of according to the purpose of study or application for the film. The LbL technique also allows the emergence of synergistic effects from the intercalated materials, which can improve and alter both physical and chemical properties of the films [5,6].

Polyaniline (PANI) is a conducting polymer that has been widely used in the preparation of thin films, chiefly due to its promising applications based on its intrinsic conductivity, chemical-environmental stability, and low production cost [7,8].

PANI-based thin films have been extensively studied together with the several types of materials [9]. Due to PANI often being found in its polycationic state, PANI multilayered thin films interlaced with PVS (poly(vinyl sulfonic acid)), a synthetic polymer with anionic characteristics, can be produced. These films have been widely used as sensors, e.g. for detecting the oxidation contents of ascorbate in human plasma [10], quantifying vitamin c [11,12], ammonia in fowl houses [7], glucose [13,14], the amino acid L-phenylalanine [15], the enzyme tyrosinase [16], among others [17].

More recently, the interest in PANI-based films interlaced with biomolecules for use as platforms to electrochemical sensors and biosensors has increased. It is believed that the use of conducting polymers may provide a larger stability to the immobilized biomolecule in the film, potentially enhancing analytical capability [9].

---

* Corresponding author at: Laboratório Interdisciplinar de Materiais Avançados, LIMAV, CCN, UFPI, Teresina, PI 64049-550, Brazil. Tel.: +55 8633215710.
E-mail address: eiras@cnpq.br (C. Eiras).

http://dx.doi.org/10.1016/j.mseb.2015.05.004
0921-5107/© 2015 Published by Elsevier B.V.

Please cite this article in press as: E.A. de Oliveira Farias, et al., Mater. Sci. Eng. B (2015), http://dx.doi.org/10.1016/j.mseb.2015.05.004

The search for biopolymers for developing electrochemical sensors and biosensors aims to replace synthetic materials, complying with sustainability procedures [18]. To this end, the development of materials using naturally-derived biomolecules and biopolymers, whose versatility, biodegradability, and non-toxicity can confer advantages over synthetic materials is an area of current intense research [19].

The gum of the cashew tree (*Anacardium occidentale* L.) is one example of a biopolymer that has been satisfactorily used as a cationic polyelectrolyte in the production of films for detecting the neurotransmitter dopamine [20,21]. Other gums from the trees *Sterculia striata* [22], *Anadenanthera colubrina* and *Sterculia urens* have also been immobilized in the form of LbL films for applications in electrochemical sensors [23]. In addition to natural gums, bioactive peptides, e.g. dermaseptin 01, found in the cutaneous secretion of *Phyllomedusa hypochondrialis* and *Phyllomedusa oreades* frogs, have also been targeted for immobilization in LbL platforms, in the production of a biosensor able to detect cells of *Leishmania chagasi* [22]. Several other biopolymers have been used in human tissue engineering [24], biocompatible and biodegradable plastics [25] and other various applications [19,26].

In view of the increasing interest applications of materials coming from natural sources, agar and carrageenan are potential biopolymer candidates [27]. These biopolymers have been successfully used in the medical area, and in the food, cosmetic, biotechnological, textile, and pharmaceutical industries [28–30]. The primary areas of use of agar and carrageenan are based on their gel-forming ability (e.g. as gellants, thickeners, and/or emulsifiers) coupled with non-toxicity. In addition, the possibility of forming a complex with bivalent ions [30] increases their potential applications. Another interesting characteristic is that the presence of sulfated groups – both in agar and in carrageenan [28] – confers a negative charge to these polymers, increasing their potential for electrostatic interactions with polycations.

The red seaweeds producing agar and carrageenan can be found widely distributed throughout the planet, chiefly in countries such as Japan, China, India, Brazil, United States, Mexico, South Africa, Morocco, Portugal, Spain, Chile, Taiwan, Philippines, Egypt, New Zealand, and Russia [31].

In Brazil, the species *Hypnea musciformis* (producer of carrageenan) and *Gracilaria birdiae* (producer of agar) have been widely explored due to their abundant distribution throughout the country's coastline. These seaweeds produce a considerable yield of the polysaccharide after extraction, however this yield can vary with of seasonality and abiotic factors [32].

On account of the possibility of using both agar (*G. birdiae*) and carrageenan (*H. musciformis*) as an anionic polyelectrolyte in forming thin films produced by the LbL self-assembly technique, the current study aimed at the preparation and characterization of multilayered films, where agar or carrageenan were interlaced together with PANI. Initially, the study of the films' physico-chemical properties was carried out, observing the influence of the parameters involved in the deposition process. Next, the feasibility of the use of these films as an active layer was verified, in the production of electrochemical sensors for the detection of Cr(VI), a genotoxic carcinogenic metal, thought to be dangerous even at low concentrations.

2. Experimental procedure

2.1. Extraction and purification of polysaccharides

The seaweeds *H. musciformes* (source of kappa-carrageenan) [33–35] and *G. birdiae* (source of agar) were collected and then submitted to sun-drying for three days. For the extraction of polysaccharides, a predetermined quantity of dried seaweed (5.0 g/200 mL water) was boiled with distilled water for 2 h. The final solution was filtered and the pH adjusted to 7.0. The polysaccharide was then recovered by means of precipitation of the filtrate in ethanol in the proportion of 1:3 (v/v). For the removal of impurities, the precipitate was washed with ethanol and acetone, and then dried under air flow.

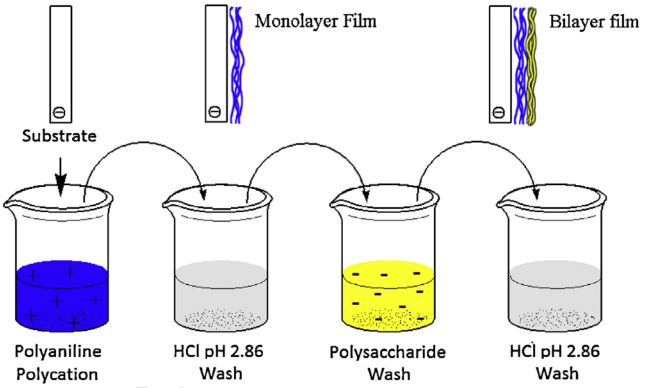

Fig. 1. Illustration of the deposition method of LbL films.

2.2. Preparation of solutions used in the formation of LbL films

Polyaniline (PANI) was obtained in the form of emeraldine base through chemical synthesis [36]. The PANI solution used in the deposition of films was prepared from a stock solution of the emeraldine base (0.47 g), solubilized in 25 mL of dimethylacetamide (DMAc), and kept overnight under stirring. Next, the solution was filtered and diluted in HCl 1.4×10^{-3} mol L^{-1} (pH 2.66) at the concentration of 0.23% (v/v). The solution of poly(vinyl sulfonic acid)–PVS (Aldrich), used in the deposition of films, was prepared in the concentration of 40 μL/100 mL (0.04%), using as a solvent HCl 1.4×10^{-3} mol L^{-1}; whereas the aqueous solution of agar and carrageenan was prepared in the concentration of 0.1% (w/v).

2.3. Assembly of the PANI LbL films and polysaccharides of seaweeds

All films were prepared through the following procedure: initially, the previously cleaned ITO [37] was immersed into the PANI solution for 5 min. Next, the set substrate/monolayer, ITO/PANI, was plunged into the washing solution (HCl pH 2.86) for the removal of the non-adsorbed material and then the film was dried under a gentle N_2 flow. After this stage, the system ITO/PANI was plunged into the polysaccharide solution (carrageenan or agar), and also kept in this solution for 5 min, which was then washed and dried with N_2. By the end of this process, a film containing a bilayer with the ITO/PANI/polysaccharide architecture was obtained. Two architectures of bilayers were analyzed: ITO/PANI/polysaccharide and ITO/polysaccharide/PANI. This study was carried out in search of a sequence of deposition that would result in larger interactions among the polyelectrolytes, and thus a greater deposited mass. Repeating the process described above, it was possible to produce multilayer films as desired. For comparative purposes, films were also studied where the polysaccharide was replaced by the PVS constituting ITO/PANI/PVS or ITO/PVS/PANI films (see Fig. 1). Q5

2.4. Characterization

The extracted polysaccharides were characterized by infrared spectroscopy in KBr pellets using a Shimadzu 8300 FT-IR

Please cite this article in press as: E.A. de Oliveira Farias, et al., Mater. Sci. Eng. B (2015), http://dx.doi.org/10.1016/j.mseb.2015.05.004

spectrometer. The analysis of zeta potential and Molecular weight (Mw) were performed by Light Scattering on a Malvern Zetasizer Nano ZS Model 3600 using a 633 nm laser in a fixed scattering angle of 173°. Each sample was measured in triplicate and described as mean ± SD ($n = 3$). The sulfate content in carrageenan and agar was obtained by inductively coupled plasma optical emission spectrometry (ICP-OES) (Spectro, model across).

The LbL films were electrochemically characterized by CV, UV–vis spectroscopy, and s for the morphology AFM was used. The cyclic voltammograms were obtained with the aid of an AUTOLAB model PGSTAT 128N potentiostat/galvanostat, and an electrochemical cell with a 10 mL capacity. A saturated calomel electrode (SCE) was used as a reference electrode for all measurements. As a counter-electrode, we used a platinum plate measuring 2.00 cm^{2}. The LbL self-assembled film deposited on ITO-coated glass substrates (area 0.35 cm^{2}), was used the working electrode. As a supporting electrolyte, HCl 0.10 mol L^{-1} was used. In the case of UV–vis spectroscopy analyses, the films were deposited on common glass substrates and the formation of the bilayers was monitored by using a SHIMADZU UV-1800 spectrophotometer.

Representative films were examined using AFM. Analysis was carried on the samples in vibrating (tapping) mode in air. Imaging was performed using a TT-AFM instrument from AFM Workshop (Signal Hill, CA, USA), equipped with an scanner with a scan range of approximately 15 × 15 × 7 μm^{3}. Tapping mode probes with a resonant frequency around 300 kHz (AppNano) were used. Images were collected at 512 pixel resolution, both 2 × 2 μm^{2} and 4 × 4 μm^{2} areas were examined, and at least three different areas were examined per sample. Representative data are shown here. Images have been processed, analyzed and displayed using Gwyddion 2.29 software. As described elsewhere [38], roughness values depend closely on the size of the area examined. We found a very similar trend between samples for roughness values measured in the different size areas, while the absolute values comparing one size to another were quite different. The values shown here are those from 2 × 2 μm^{2} areas, and represent the root mean square roughness (Rq) values [38].

To perform the measurement of film thickness, a risk on the film with the aid of an injection needle was made thoroughly and AFM images were captured as described above at the risk region, at the interface between the film and the ITO substrate. For each film, four images were captured and the measurements were made using Gwyddion 2.29 software. We measured five areas in each image by noting the distance (height) between the film and the glass, and then calculated the mean and the standard deviation.

2.5. Electrochemical detection tests of Cr(VI)

In the chromium (VI) detection tests, a solution of 1.0×10^{-2} mol L^{-1} of potassium dichromate was used, solubilized in 0.1 mol L^{-1} HCl. The strong yellow-orange staining indicates the presence of the metal in hexavalente state. All electrochemical measurements carried out in the specification and determination experiments of Cr(VI) were accomplished in a 1.0 mol L^{-1} potassium phosphate buffer at pH 1.5 (adjusted with phosphoric acid). In this study, LbL films were used containing only one bilayer of the optimized system. First, the influence of the metal in the electrochemical cell has been studied by cyclic voltammetry. Later, the standard curve was obtained by means of differential pulse voltammetry (DPV). The LoD (limit of detection) and the LoQ (limit of quantification) were calculated by using the data obtained from this curve. Table 1 shows the optimized parameters used in determining the Cr(VI).

Table 1
Parameters optimized in determining Cr(VI).

Initial potential	0.51 V
Final potential	0.2 V
Deposition potential	0.51 V
Deposition time	10 s
Stirring	220 RPM
Stirring time	10 s
Equilibrium time	5 s
Scanning rate of the potential	5 mV s^{-1}
Scanning mode	Differential pulse
Pulse range	25 mV

3. Results and discussion

3.1. Characterization of polysaccharides

In samples of seaweeds' polysaccharides, the infrared spectra (FT-IR) analysis is normally used to acquire information on the presence of sulphate groups and 3,6-anhydrogalactose units [39]. The infrared absorption spectra for the agar and carrageenan samples can be observed in Fig. 2. Bands characteristic of C–O–C stretching vibrations of glycosidic bonds are observed at 1158 cm^{-1} and 1077 cm^{-1}.

In the spectral range between 1100 cm^{-1} and 1000 cm^{-1} we observed spectral differences between the three main types of carrageenan (kappa, iota and lambda), which enables the use of FT-IR also to classify them between their different types. The sharp band at 1077 cm^{-1} and 1045 cm^{-1} mainly, Fig. 2A, are characteristic of kappa-carrageenan [40].

The band at 1262 cm^{-1} indicates the existence of a large percentage of total sulfate groups in the polysaccharide's structure, also confirmed by the presence of bands at 920 and 847 cm^{-1} (this band also indicates the presence of kappa-carrageenan [70]), attributed respectively, to the 3,6-anhydrogalactose and galactose-4-sulfate units [41]. For the polysaccharide agar (Fig. 2B), the presence of a less intense band at 1250 cm^{-1} suggests the existence of a small percentage of sulfate groups in the polysaccharide's structure.

The zeta potential of the agar and carrageenan solution was measured as approximately −30.4 and −42.0 mV, respectively. For agar and carrageenan, the molecular weight was estimated at 1.4×10^{3} kDa and 5.6×10^{3} kDa, respectively. The sulfate content found in carrageenan and agar was 8.80% and 2.73%, respectively.

3.2. Electrochemical characterization by cyclic voltammetry

For a better understanding of the existing synergic effect among the interlaced materials in the structure of bilayers, initially, we carried out individual studies of each one of them. Fig. 3 shows the cyclic voltammograms obtained for the non-modified ITO, i.e., with no deposited material, and ITO modified with monolayers of both agar and carrageenan. The voltammograms obtained showed that none of the natural polysaccharides alone is electroactive under in the conditions studied, as both exhibited the same behavior observed for the non-modified substrate. The small increase in the values of current due to the adsorption of a monolayer of these polysaccharides may be explained as an increase of the active area of the electrode surface, due to the presence of agar or carrageenan over the substrate.

In the next step, bilayer films including PANI were prepared together with the polysaccharides used as anionic polyelectrolytes, in two distinct deposition sequences – ITO/PANI/polysaccharide and ITO/polysaccharide/PANI – aiming to study the effect of the deposition order on the electrochemical response of the films, Fig. 4. For comparative purposes, the response of the ITO/PANI-only film is also shown.

Please cite this article in press as: E.A. de Oliveira Farias, et al., Mater. Sci. Eng. B (2015), http://dx.doi.org/10.1016/j.mseb.2015.05.004

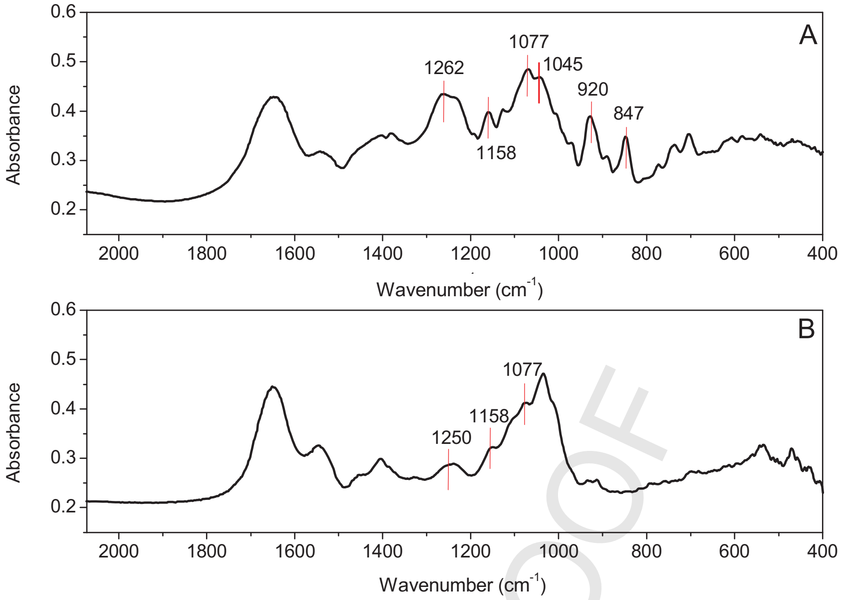

Fig. 2. FTIR spectra obtained for the polysaccharides used: (A) carrageenan and (B) agar.

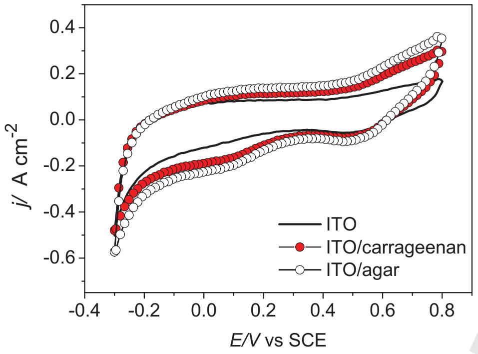

Fig. 3. Cyclic voltammograms obtained for the ITO and for the ITO modified by the deposition of a monolayer of agar, ITO/agar, or carrageenan, ITO/carrageenan. All measurements were carried out in HCl 0.1 mol L^{-1} at ν = 50 mV s^{-1}.

All voltammograms shown in Fig. 4A and B exhibit redox processes characteristic of the conducting polymer, PANI, which are well-described in the literature [36]. During the direct scanning, one can observe the transition from the leucoemeraldine salt form (LES) of PANI, into the emeraldine salt (ES) at +0.15 V (E_{ox1}) and, later on, the conversion from the ES form into the pernigraniline base (PGB), which occurs at +0.64 V (E_{ox2}) giving in total two oxidation peaks. During reverse scanning, the voltammograms show two reduction peaks, resulting from the change from PGB into ES, in the region at approximately +0.6 V (E_{red1}) and the transition from ES into LES at −0.02 V (E_{red2}). Fig. 4C shows the redox mechanism of PANI [69].

The results revealed that none of the polysaccharides employed in the formation of PANI-based films suppress the electroactivity of this material, independent of the deposition sequence adopted, Fig. 4. This same effect was previously observed for PANI films prepared together with the cashew tree gum (*Anac. occidentale*) [21] and also for films of POMA, a derivative of polyaniline, interlaced with gums of the trees *S. striata* and *Anadenanthera macrocarpa* [42].

Also in Fig. 4, it is possible to observe the effect of the deposition sequence in forming the bilayered films showing a direct relationship with the current response obtained for the films. For both polysaccharides studied, larger current density values were obtained for the films that had the PANI monolayer adsorbed as an outer layer, i.e., ITO/agar/PANI and ITO/carrageenan/PANI films, Fig. 4A and B, respectively. In both cases, it was observed that the previous deposition of a polysaccharide monolayer (agar or carrageenan) provides more active sites for the adsorption of PANI in the next step, reflected by the higher current density observed for the film when prepared in this deposition sequence. Thus, a larger quantity of polyaniline is adsorbed during the same deposition time, because of the previous modification of ITO with the polysaccharide.

In Fig. 4, it can also be observed that the effect of the deposition sequence is greater for the case in which the polysaccharide used was agar, Fig. 4A. In fact, the deposition after that of a PANI layer showed no significant increase in PANI electrochemical response, compared to the PANI alone. This is in contrast to the carrageenan, whose deposition increased the response of the PANI, whether it was deposited first or second, while in this cases as well, deposition of the biomolecules before the PANI lead to a greater current in the PANI response. Furthermore, ITO/agar/PANI films showed larger current density values in the electrochemical responses compared to the ITO/carrageenan/PANI film, in addition to an excellent definition of the redox processes of PANI. This improvement in the definition of redox processes (particularly for the second process as +0.64 V) recorded in the voltammogram occurs for both deposition sequences assessed, providing a decrease in the capacitive current in the film/electrolyte interface, enabling a signal more indicative of Faraday current, thus reflecting a better definition of the intrinsic redox processes of PANI, Fig. 4A. This result could be related to a higher level of deposition of the ITO/agar/PANI film compared to the carrageenan-containing one, as discussed further in Section 3.4 in relation to the results from AFM.

3.2.1. *Influence of polysaccharides in the films' electrochemical stability*

It is important that the LbL systems developed are stable in order to enable their application in electrical or electrochemical devices, e.g. sensors. The electrochemical stability is very important, as it will directly influence the reproducibility and usability of the sensor.

There are a large number of applications for sensors in the literature made up of PANI films; however, their commercialization is still a challenge, due to the aging effect, the low electrochemical

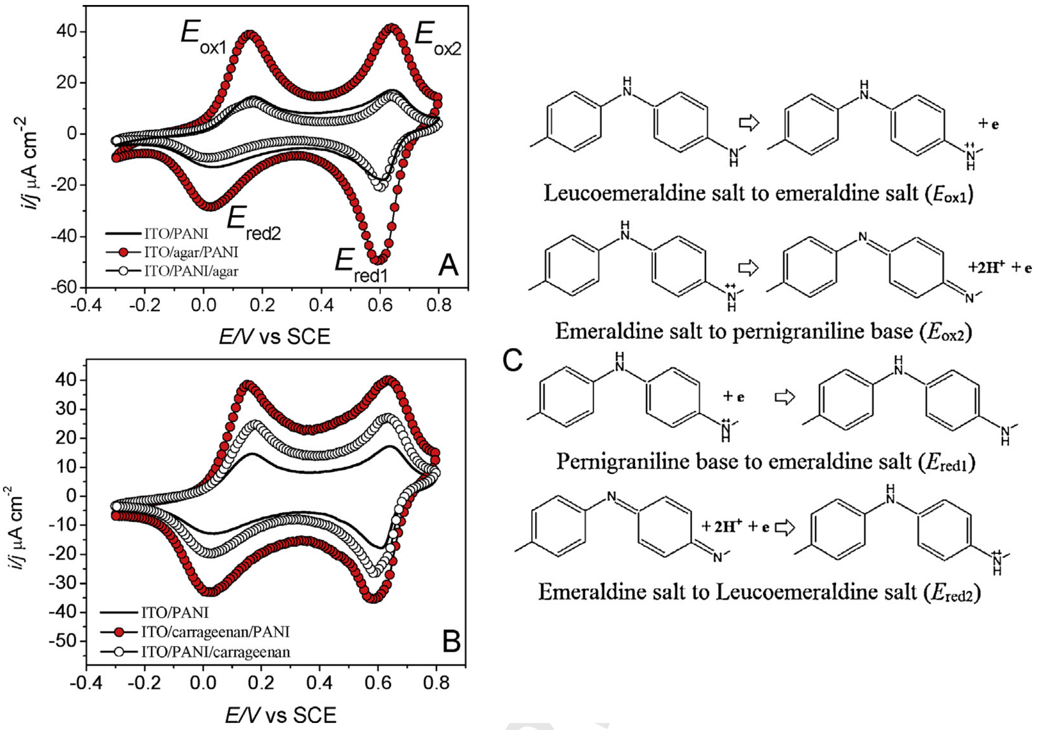

Fig. 4. Cyclic voltammograms obtained for bilayer films formed by PANI and polysaccharides, deposited on ITO, in two distinct deposition sequences; (A) ITO/agar/PANI and ITO/PANI/agar, (B) ITO/carrageenan/PANI and ITO/PANI/carrageenan. (C) Shows the mechanism of PANI (adapted from [69]). All measurements were carried out in HCl 0.1 mol L^{-1} at ν = 50 mV s^{-1}.

stability of PANI, and the lack of optimized deposition techniques [43].

We sought to assess whether the interlaced polysaccharides together with PANI in the form of LbL films could improve the electrochemical stability of the conducting polymer. For these studies, the bilayered films were prepared by adsorbing PANI as the outer layer (ITO/agar/PANI and ITO/carrageenan/PANI) – Fig. 5 – as an optimized system. For comparative purposes, the electrochemical stability of an ITO/PVS/PANI bilayered film was also studied, Fig. 5A, in which the polysaccharides were replaced by polyvinyl sulfonate – PVS, an anionic and synthetic polyelectrolyte, commonly used in forming PANI-based LbL films. The ITO/PVS/PANI films were prepared under the same conditions employed for the films of polysaccharides/PANI. These tests of electrochemical stability were carried out with one-bilayer films only, and data was collected for 25 subsequent cycles for all cases.

Fig. 5 shows the voltammograms obtained in the electrochemical stability test of the films developed. It can be observed that as PANI is repeatedly cycled in an acid medium, an intermediate redox couple grows in the region at 0.4 V vs. SCE, which is related to the irreversible acidic degradation of PANI. This redox couple is characteristic of benzoquinone and hydroquinone groups present in the degradation products of PANI [43,44].

The bilayered films formed by means of the joint immobilization of PANI with the polysaccharides (ITO/agar/PANI and ITO/carrageenan/PANI, Fig. 5B and C, respectively) show a reduction in the acid degradation process of polyaniline and increase the stability of their redox processes peaks, when compared to the ITO/PVS/PANI film, Fig. 5A. In view of these results, we can infer that the polysaccharides promote an increase in the polyaniline stability during the successive scans in an acid medium. This same effect promoted by the presence of agar and carrageenan in the film was also described for multilayered films of PANI and cashew tree gum (*Anac. occidentale*) [21] and films of POMA with gums of *S. striata* and *Anad. macrocarpa* [42]. As also observed in studies using other natural polysaccharides [21,42], the agar and carrageenan work as a type of antioxidant for polyaniline, since it reduces the acid degradation effect observed for PANI, which occurs because of the high polarization potential and the electrolyte HCl employed. It is important to note that the antioxidant activity of polysaccharides from seaweed may vary depending of the molecular weight, composition of functional groups and monosaccharides present [45,46]. The main groups of these polysaccharides that have shown good antioxidant activity are: sulfate ester, uronic acid, amine and hydroxyl [45], phosphate groups [47] and sulfate groups [46–48]. It is possible that the sulfates and hydroxyl groups present in both the agar and carrageenan are the responsible for the reported effects.

Another interesting result observed was that, for the ITO/agar/PANI film, Fig. 5B, there was no dislocation of the potentials of the process II′ of PANI with increasing number of cycles, as was observed for the other systems, Fig. 5A and C. This effect may be related to the electrochemical stability of the films. The fact that these shifts were not observed for the ITO/agar/PANI film indicates that this film has a higher electrochemical stability than the others, since these shifts in potential may be related to the readjustment of the film/electrolyte interface during the successive scans.

In order to quantitatively investigate the stability of the films, the percentage of loss in intensity of the current peaks for each process of PANI, as a function of the number of cycles was plotted in Fig. 6.

Fig. 6 confirms that it is advantageous to use natural polysaccharides for building stable films with PANI, compared to use of PVS as the polyanion. For the films built using polysaccharides, all anodic and cathodic processes of PANI had a smaller percentage of current loss, when compared to ITO/PVS/PANI films. The decrease in current loss between the different films also increased with the number of cycles carried out. In the case of the first oxidation process of PANI (I), Fig. 6A, the ITO/carrageenan/PANI film lost only 3% of current, whereas the ITO/agar/PANI and ITO/PVS/PANI films lost

Please cite this article in press as: E.A. de Oliveira Farias, et al., Mater. Sci. Eng. B (2015), http://dx.doi.org/10.1016/j.mseb.2015.05.004

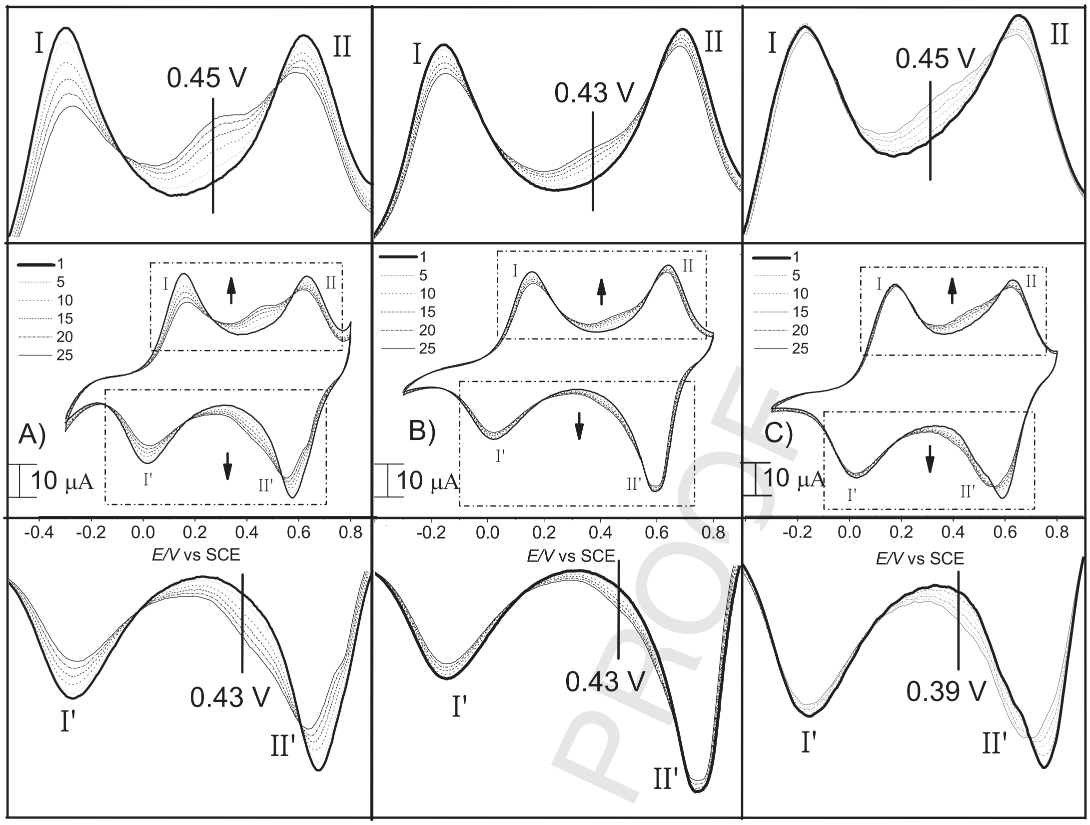

Fig. 5. Electrochemical stability studies. Results show subsequent cyclic voltammograms obtained during the cycling, which was carried out 25 successive times in each case. Only 6 representative curves are shown in each case, for clarity (A) ITO/PVS/PANI, (B) ITO/agar/PANI, and (C) ITO/carrageenan/PANI.

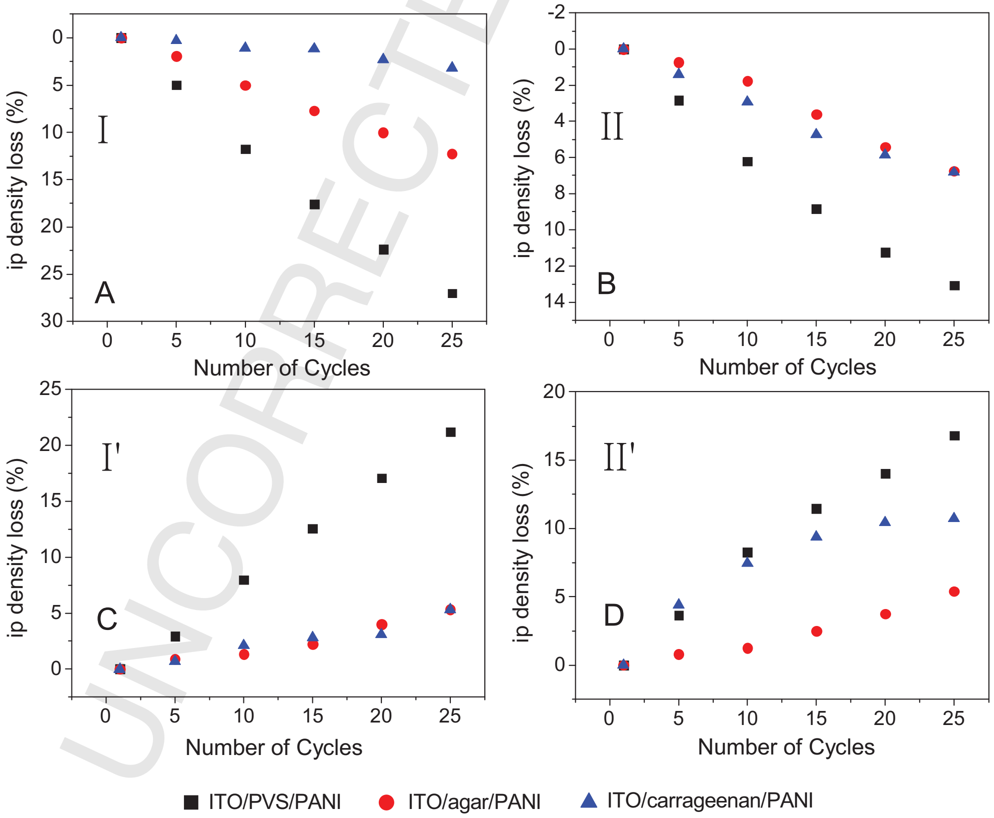

Fig. 6. Peak current (*ip*) density loss in function of the number of cycles for the anodic processes of PANI (A and B) and its respective cathodic processes (C and D).

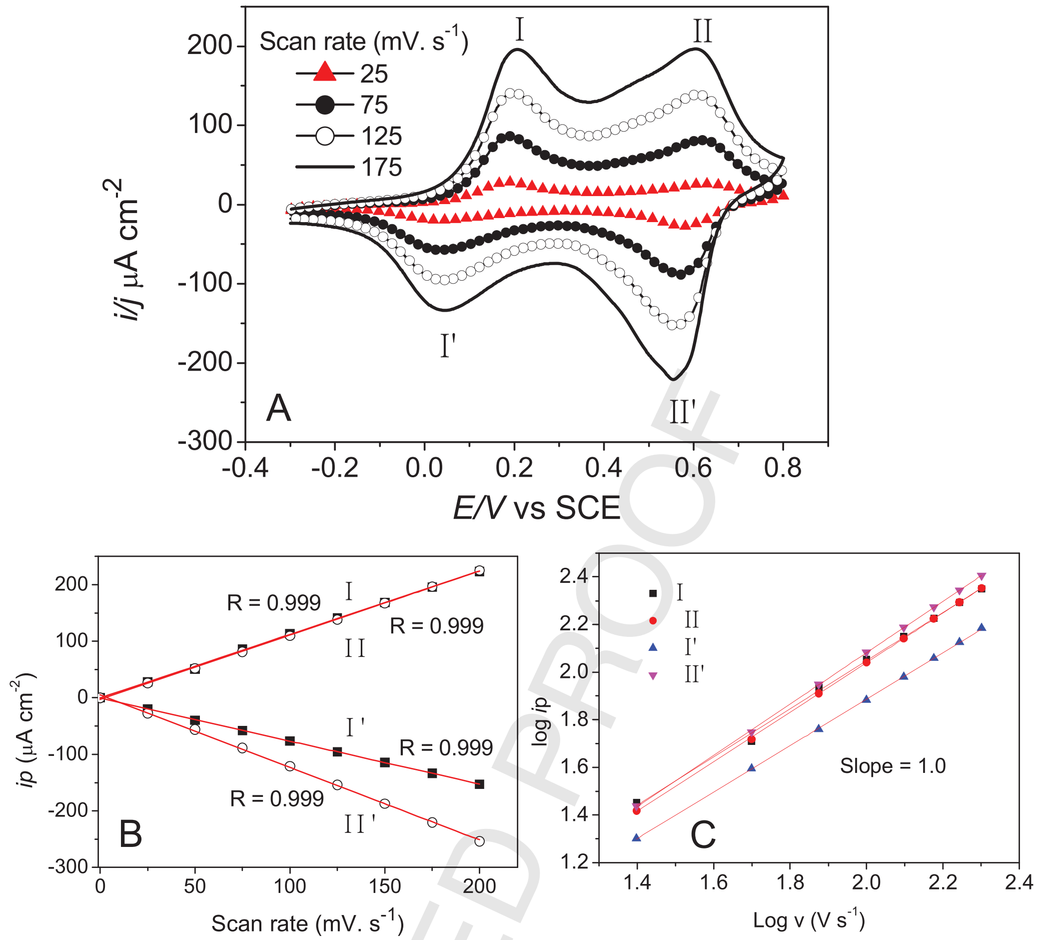

Fig. 7. (A) Cyclic voltammograms obtained for the ITO/agar/PANI film under different scanning rates and (B) linear correlation observed for the values of current in function of the rates studied (ν = 25, 50, 75, 100, 125, 150, 175 and 200 mV s^{-1}). (C) Shows linear relationship between log ν and log ip. All measurements were carried out in HCl 0.1 mol L^{-1}.

around 12% and 28%, respectively. For the second oxidation process (II), Fig. 6B, the films made up of polysaccharides lost 6% of their current, whereas the film containing PVS decreased the current up to 13% of its total. In the case of cathodic processes, in the reduction process I′, Fig. 6C, there was a peak loss of up to 5% when the polysaccharides were employed. However, when these polysaccharides were replaced by PVS, the peak current loss was up to 23%. The stability of the cathodic process II′, Fig. 6D, was more affected by the use of carrageenan and PVS, and this lead to peak intensity loss up to 17%, after 25 scanning cycles. Through this analysis, we can infer that the ITO/polysaccharides/PANI films were 2 or 3 times more stable than the ITO/PVS/PANI films.

3.2.2. Studying the scanning rate and the influence of the number of bilayers on the films' electrochemical response

The study of the scanning rate effect for the ITO/agar/PANI film is shown in Fig. 7A. The linear relationship between the scanning rate and peak current (ip vs. ν) for each redox process of PANI (I, I′, II and II′) is shown in Fig. 7B. This linearity confirms the film's thermodynamic stability within the experimental conditions probed [49]. This correlation further suggests that the transmission of charges in the interface electrode/solution occurs in a regular manner and that the electrochemical processes occur by charge transfer processes, since the ratio ip vs. ν showed a correlation coefficient, R = 0.999 for all cases [50,51]. The results also suggested that PANI is strongly adsorbed on the surface of the electrode, since the ratio of log ν vs. log ip showed a slope of 1.0 for all cases (see Fig. 7C) [52]. It is worth pointing out that similar results were obtained when, instead of using agar, we used carrageenan (results not shown herein).

So far, the data described were obtained with single bilayers. In addition films produced by multiple deposition cycles, i.e., multilayer films, were studied. In Fig. 8, it is possible to observe the influence of the number of bilayers in the films' electrochemical response. For the ITO/agar/PANI film, it was observed that the current increases with the number of deposited bilayers. However, for the ITO/carrageenan/PANI film, after the third bilayer, there seems to be a saturation of the system, shown through the decrease in current density obtained for the film prepared with five bilayers.

3.3. Ultraviolet–visible (UV–vis) spectroscopic characterization

PANI in its emeraldine salt form, which was used herein, showed two main absorption bands under the conditions used, one at 335 nm and another at 640 nm. The band observed at 335 nm is attributed to the transition π–π^* of benzene rings, whereas the band at 640 nm is attributed to the transition n–π^* of quinoid rings of the conducting polymer [53,54]. The self-assembled films proposed also showed bands at 400 and 900 nm, and this latter was observed only in the case of films made up of carrageenan and PANI. Both absorption bands are attributed to the polaronic transitions in PANI, confirming their conducting characteristics [55,56].

The absorption band at 640 nm was used as a measured of film thickness because it was highly intense and present in all cases. Thus, we used this band in the UV–vis absorption spectrum

Please cite this article in press as: E.A. de Oliveira Farias, et al., Mater. Sci. Eng. B (2015), http://dx.doi.org/10.1016/j.mseb.2015.05.004

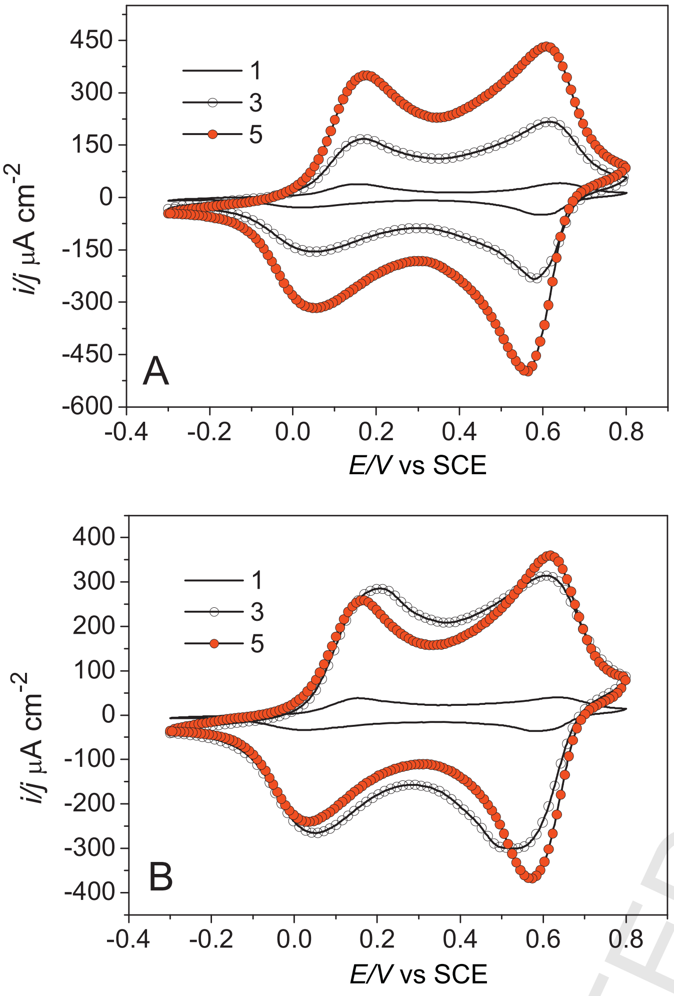

Fig. 8. Response obtained for the films of (A) ITO/agar/PANI and (B) ITO/carrageenan/PANI, prepared from 1, 3, and 5 bilayers. All measurements were carried out in HCl 0.1 mol L^{-1}.

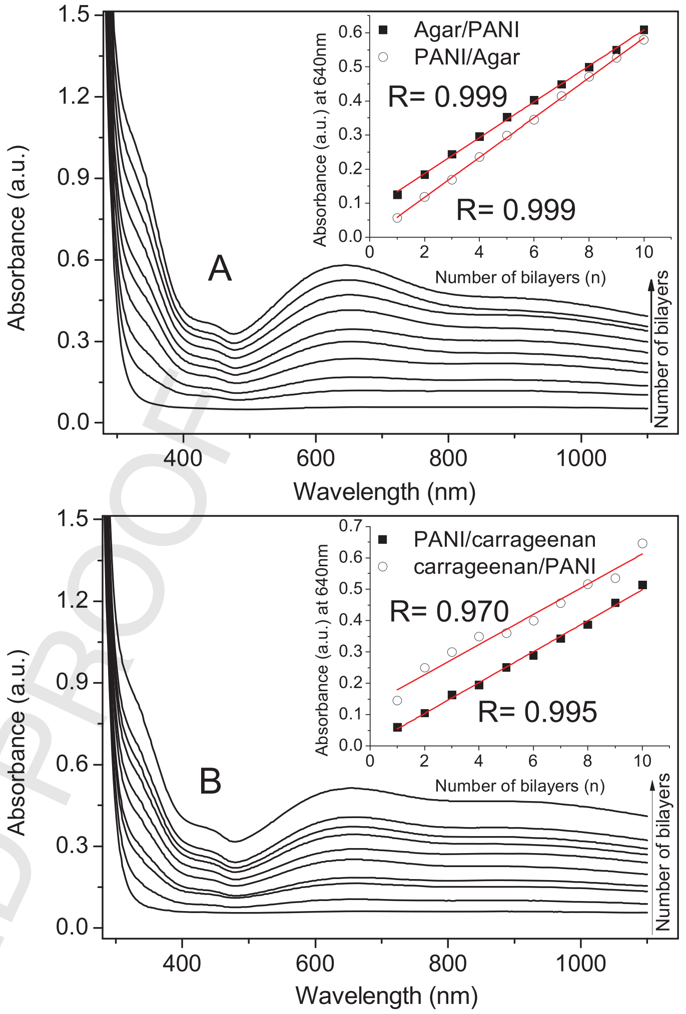

Fig. 9. UV–vis data on the formation of thin films of (A) agar/PANI and (B) carrageenan/PANI on glass slides with $n = 1$–10. The inset curves show the relationship between absorbance at 640 nm and the number of adsorbed bilayers (n) for the two deposition orders – polysaccharide/PANI and PANI/polysaccharide.

to follow the self-assembly of the films, correlating the maximal absorbance value of this peak, with their thickness via the Beer–Lambert law [57]. It is worth pointing out that UV–vis studies were carried out using glass slides rather than ITO-coated glass, and in this work we assumed that there was no significant difference in the deposition of the films on the two films.

Fig. 9A shows the spectra obtained for the agar/PANI films with increasing numbers of adsorbed bilayers (ranging from 1 to 10). In the inset of Fig. 9A, the linear relationship between the absorbance at 640 nm and number of adsorbed bilayers (n) is exhibited, for both the PANI/agar and agar/PANI architectures. In Fig. 9B, the corresponding spectra for the carrageenan/PANI system are shown along with the inset showing the relationship of (n) with the absorbance at 640 nm for both systems, carrageenan/PANI and PANI/carrageenan.

In accordance with the results already shown by cyclic voltammetry, the UV–vis spectroscopy measurements showed that the deposition sequence with larger absorbance values was that in which the conducting polymer was adsorbed after previous modification of the substrate with the polysaccharide, in both the cases of agar and carrageenan. In the case of the agar-containing films, it seems that this effect decreased in films with larger numbers of bilayers (see inset in Fig. 9A). Eventually, after 10 layers, the total amount absorbed was practically identical for the two geometries. In the case of the carrageenan-containing system, the amount of material in the two types of films did not approach each other, but the large difference seen between the methods of deposition of the polysaccharide first or second, was not reproduced after the first cycle. It appears that in this case, one layer of polysaccharide is sufficient to increase the amount of PANI that is absorbed in each step, and further bilayers effectively each contain similar masses of material irrespective of the deposition order.

For the agar and PANI film self-assembly, it was observed that the growth process in this system was highly regulated, i.e., the quantity of adsorbed material was virtually the same in each adsorption cycle (see the correlation index (R) in the inset of Fig. 9A). This same behavior was previously reported for films made up of PVS and PANI [7]. In the case of films prepared under the use of carrageenan and PANI, Fig. 9B, a smaller linear correlation (R) was observed for the deposition sequence of carrageenan/PANI (see inset of Fig. 9B).

Regarding the results obtained by cyclic voltammetry and UV–vis, we can infer that the adsorption mechanism and the interaction occurring between the films of agar and PANI are different from those that occur in films of carrageenan with PANI. We believe that the different levels of charges existing between polysaccharides may be influencing in the charge compensation mechanism [58], during the preparation of these films.

Table 2
Average roughness data calculated for the films from the AFM results.

Sample	Mean Rq (standard deviation)/nm	Texture difference compared to ITO
ITO	2.5 (0.1)	–
PANI monolayer	2.4 (0.3)	–
Carrageenan monolayer	2.1 (0.2)	–
Agar monolayer	4.3 (0.3)	+
1 Bilayer of PANI/carrageenan	3.2 (0.4)	++
1 Bilayer of carrageenan/PANI	5.2 (1.0)	+++
2 Bilayers of carrageenan/PANI	4.7 (1.4)	+++
3 Bilayers of carrageenan/PANI	5.6 (2.2)	+++
1 Bilayer of PANI/agar	2.1 (0.1)	++
1 Bilayer of agar/PANI	6.6 (0.7)	+++
2 Bilayers of agar/PANI	10.0 (2.8)	+++
3 Bilayers of agar/PANI	9.8 (6.2)	+++

3.4. Morphological characterization by atomic force microscopy (AFM)

Atomic force microscopy was used to examine the films produced, and to quantify their surface roughness. The first experiments, as controls, studied the substrate, ITO, and then monolayers of PANI, carrageenan and agar alone. Representative images are shown in Fig. 10. ITO, indium tin oxide, electrodes exhibit a well-known and highly characteristic microstructure, which has been observed by AFM many times before, for example in EATON and WEST [38]. This structure, shown in Fig. 10A, consists of somewhat flat "islands"; each covering areas of 100 nm^2 up to 1 μm^2 made up of many small (<40 nm) globular grains, which stand above similar globular grains at a lower level. The structure of the PANI monolayer alone was recognizably very similar to that of untreated ITO, although it did exhibit some larger globular features not seen on the ITO alone (Fig. 10B). The structure of the carrageenan films were also very similar to that of the ITO, possibly even more so than the PANI alone (10C). On the other hand, the agar monolayer exhibited a quite different structure, with the "island" structure somewhat disguised (presumably due to deposition of agar filling in the spaces between the islands), and more randomly dispersed globules, of larger diameter than those seen on ITO randomly distributed across the surface. Overall, the carrageenan and PANI films were quite similar to the ITO, while the agar monolayer showed a distinct morphology. We interpret this as indicating that the PANI and carrageenan monolayer films deposited considerably less material on to the ITO surfaces. Roughness values backed this observation up, with 2 × 2 μm^2 areas showing similar values for ITO, PANI and carrageenan, while the number for agar was almost twice that of ITO (Table 2).

Once we begin to look at bilayers, we see quite different results (Fig. 11). Fig. 11 shows representative images of bilayers consisting of PANI/carrageenan, carrageenan/PANI, PANI/agar, and agar/PANI. In combination with the roughness values in Table 2, these images are quite instructive. In general, the bilayer images showed more differences compared to the ITO substrate than the monolayers, with many areas showing larger globular features, and in many images the "island" structure of ITO completely absent. In the case of the films where the polysaccharide was applied first, additional features are seen, namely very large clusters of globular features spread across the film. These can be seen in Fig. 11B and D. In both of these cases, in the height images, the features appear as large white features on this scale, and the height color scales for these images are already much higher than those of the images of films in which PANI was deposited first (Fig. 11A and C).

This shows the deposition of increased amounts of material in these films. This observation is also reflected in the roughness values, the polysaccharide/PANI films showed average roughness values of 5.2 nm and 6.6 nm for carrageenan and agar, respectively, compared to 3.2 nm and 2.1 nm for the films where the PANI was deposited first. The increased roughness undoubtedly stems from the presences of these large polymer aggregates across the surface. Representative images of multi-bilayer films are shown in Fig. 12. At first glance, there is no particular trend apparent in these images, the multi-bilayers appearing to exhibit similar morphology to the single bilayer films. However, the roughness in the agar-containing multilayer films increases beyond one bilayer, unlike the multilayer carrageenan-containing films. This observation correlates somewhat with the images, which showed increased numbers of the large globular aggregates on the agar multilayers, as the number of layer increased (see Fig. 12D–F).

Overall, the studies of film topography and roughness by AFM support the previous conclusions, drawn from the electrochemical results, that the deposition order strongly affects the amount of material absorbed: deposition of the polysaccharide before the PANI lead to greatly increased amounts of material deposited. Furthermore, the use of the two polymers together (polysaccharide and PANI), was a superior deposition method compared to monolayer deposition alone, lending support to the proposal that the use of alternating layers (LbL deposition), can give a synergistic effect, increased deposition, and improving film structure. On this last point, it is interesting to note that AFM showed that although for multilayers, the whole of the ITO electrode surface was covered, there was quite an uneven distribution of material on the size scale probed. This is in sharp contrast to UV–vis results, which show an extremely linear, and reproducible deposition as the number of layers increased. Presumably, this is due to the small areas probed by the AFM imaging. While on the scale of these AFM images, the deposition appears uneven, over the whole slide (whose area was typically some 107 times larger than the images shown here), the deposition of these polymeric aggregates must have been very even and highly reproducible, since UV–vis results suggest almost identical masses were deposited in each cycle.

The thickness of the films also was determined by AFM. Films containing 4 bilayers of ITO/agar/PANI or ITO/carrageenan/PANI presented thickness about 27.1 ± 5.2 nm and 31.3 ± 7.3 nm, respectively. Since the films produced showed a linear increase with increasing number of bilayers (Fig. 9), we can estimate that the ITO/agar/PANI and ITO/carrageenan/PANI films grew about, 7 nm and 8 nm per bilayer adsorbed, respectively.

3.5. Applications in sensors for detecting chromium (VI)

Chromium is one of the most widely used elements in industrial such as coating and galvanoplasty, manufacturing of alloys, the dying industry, tanning of hides, and wood treatment [59]. This metal can be found in various oxidation stages, and the most common are Cr(III) and Cr(VI) [60]. Cr(III) is poorly soluble and regarded as an essential micronutrient in biological activity, whereas Cr(VI) is quite soluble and highly toxic, even at low concentrations, and it can even cause carcinogenic effects [61]. In the literature, there are various works on the use of PANI for removing Cr(VI) from an aqueous medium [62–64], due to the environmental importance of this metal. However, there are few works on the use of this polymer in the detection and direct electrochemical quantification of Cr(VI). In this sense, we proposed to assess the efficiency of films developed herein as electrochemical sensors for detecting Cr(VI), Fig. 13.

In Fig. 13A, it is possible to observe the results obtained by cyclic voltammetry, where aliquots of Cr(VI) were added to the electrochemical cell and the response of the ITO/agar/PANI film was observed. As there is oxidation of PANI at 0.19 V (the first oxidation process which is related to the transition from the leucoemeraldine form to emeraldine), Cr(VI) is bound to PANI, causing a new voltammetric wave around 0.35 V, which can be attributed to the

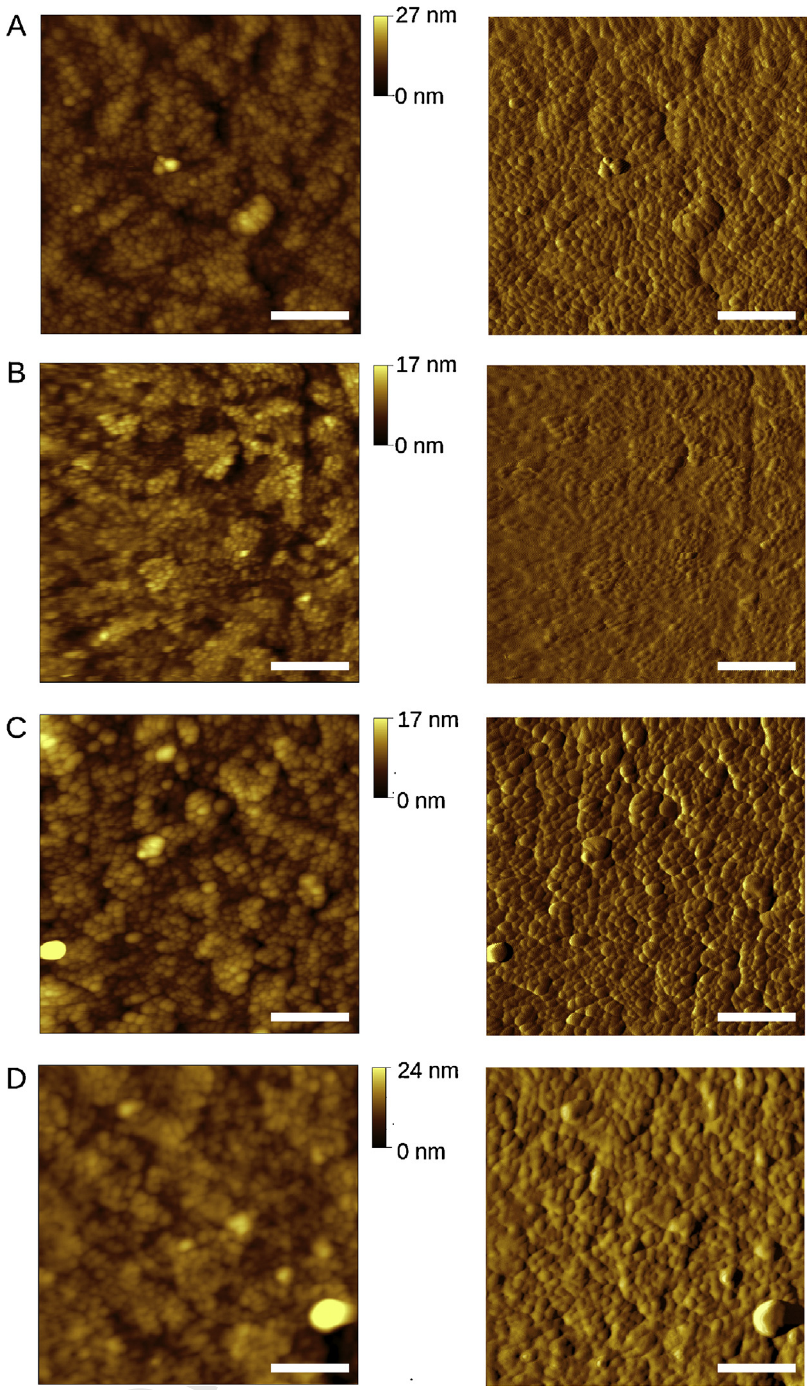

Fig. 10. Intermittent contact mode AFM images of substrate and monolayers. Left images are height images and the right images are amplitude images. (A) ITO and modified ITO with monolayer of (B) PANI, (C) carrageenan, and (D) agar. All images cover a range of 2 × 2 μm^2 in *x* and *y*. The scale in lower right corner corresponds to 500 nm.

presence of Cr(VI). With the increase of the metal's concentration, it could be observed that there was a decrease of the first cathodic peak of the conducting polymer and, consequently, the increase of peak current observed in the region 0.35 V. These effects were not observed when only 0.1 mol L^{-1} HCl (the medium of solubilization of the Cr(VI)) was added.

In the inset of Fig. 13A the values of current obtained at 0.35 V are shown as a function of the concentration of Cr(VI) present in the cell, showing a linear behavior, thus demonstrating that the film has a potential for determining the concentration of the metal in an aqueous medium.

In a next stage, the determination of Cr(VI) was tested by a more sensitive technique, e.g. differential pulse voltammetry (DPV). Fig. 13B shows the voltammograms obtained for the ITO/agar/PANI films in the presence and absence of the metal, where it was observed that the film does not show any redox process in the potential interval studied. Upon adding Cr(VI) to the cell, there was an increase of the peak current as a function of the increase of the Cr(VI) concentration in the cell, Fig. 13B, so that this relationship was linear, Fig. 13C. It is important to point out that concentrations higher than 50 μmol L^{-1} are outside the system's linearity, due to the occurrence of saturation at the electrode surface. The LoD

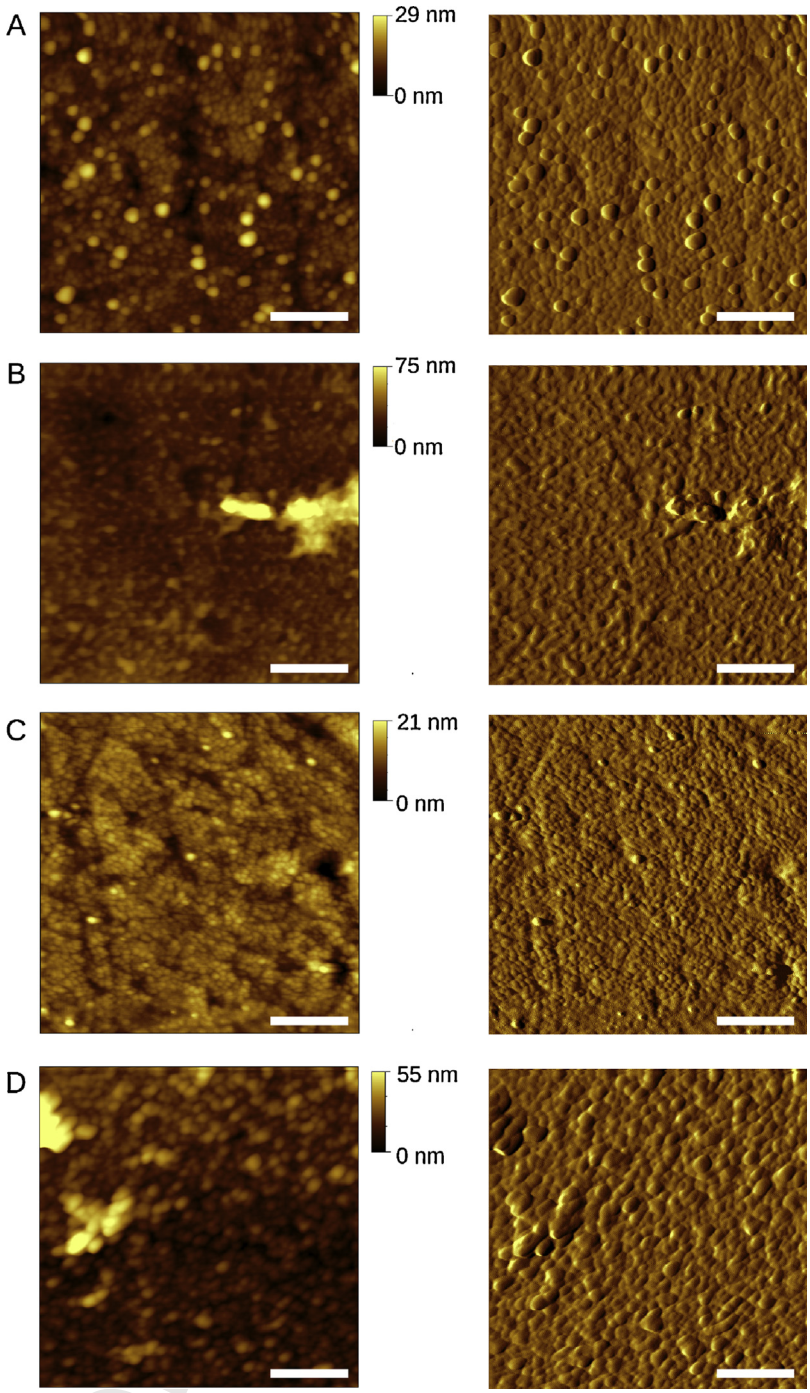

Fig. 11. Intermittent contact mode AFM images of 1 bilayer films of (A) PANI/carrageenan, (B) carrageenan/PANI, (C) PANI/agar, and (D) agar/PANI. Left images are height images and the right images are amplitude images. All images cover a range of 2 × 2 μm^2 in *x* and *y*. The scale in lower right corner corresponds to 500 nm.

Table 3

Q8

Electrode used	LoD (mol L^{-1})	Linear range (mol L^{-1})	Reference
ITO/agar/PANI LbL film	2.48×10^{-6}	2.48×10^{-6} to 50.0×10^{-6}	This work (Fig. 13C)[a]
ITO modified with gold nanoparticles	0.1×10^{-6}	0.5×10^{-6} to 50.0×10^{-6}	Tsai and Chen [65]
Electrolyte membrane insulator semiconductor sensor (prepared by deposition of tributylphosphate)	1.0×10^{-5}	1.0×10^{-4} to 1.0×10^{-1}	Zazoua et al. [66]
Screen-printed electrodes modified with L-3,4-dihydroxyphenylalanine	0.11×10^{-6}	0.19×10^{-6} to 2.4×10^{-6}	Banerjee and Sarkar [67]
Mercury electrode modified with Cu–adenine complex	0.04×10^{-6}	0.10×10^{-6} to 2.3×10^{-6}	Safavi et al. [68]

[a] Calculated based on the analyses carried out with the ITO/agar/PANI films.

Please cite this article in press as: E.A. de Oliveira Farias, et al., Mater. Sci. Eng. B (2015), http://dx.doi.org/10.1016/j.mseb.2015.05.004

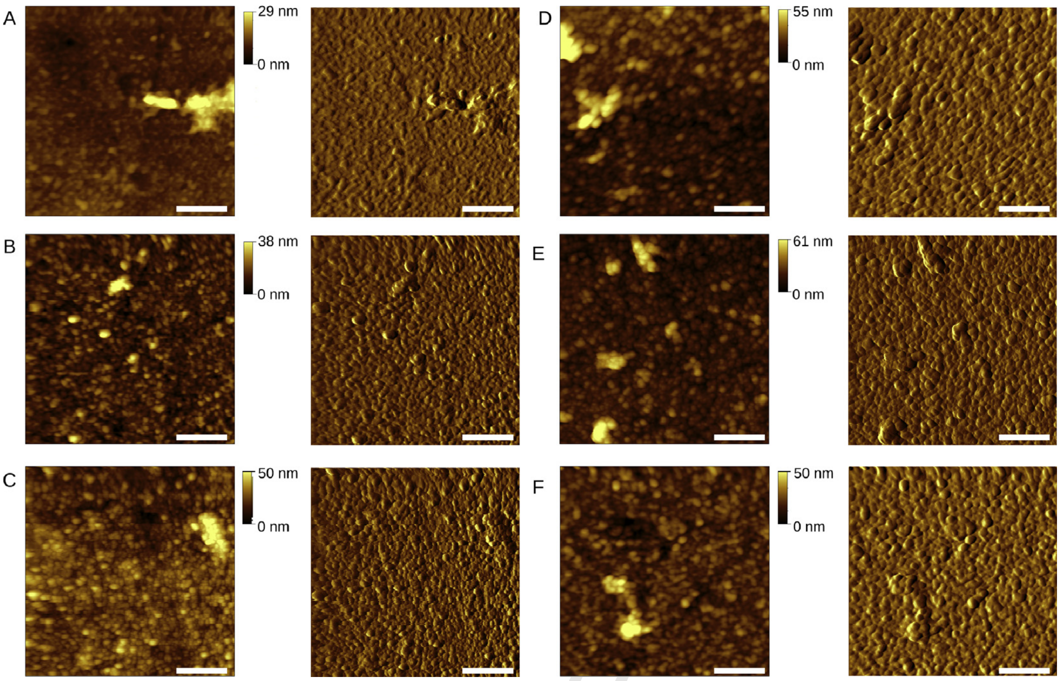

Fig. 12. Intermittent contact mode AFM images illustrating growth of multilayer films. Left: carrageenan/PANI films in (A) 1, (B) 2, and (C) 3 bilayers, and right: films of agar/PANI in (D) 1, (E) 2, and (F) 3 bilayers. Each pair shows a height image on the left, and amplitude image on the right. All images cover a range of 2 × 2 μm^2 in *x* and *y*. The scale in lower right corner corresponds to 500 nm.

(limit of detection) and the LoQ (limit of quantification), calculated through the analytic curve obtained (Fig. 13C), were 2.48 $\mu mol\ L^{-1}$ and 7.51 $\mu mol\ L^{-1}$, respectively. In Table 3 it is possible to observe the LoD calculated for the calibration curve obtained, in comparison with other electrochemical sensors of chromium (VI) found in the literature.

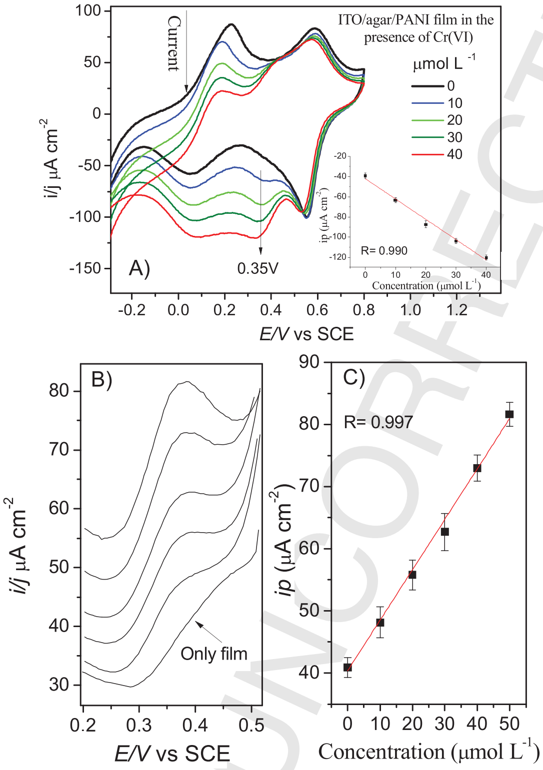

Fig. 13. Cr(VI) detection by an ITO/agar/PANI film by different techniques (A) cyclic voltammetry at $\nu = 50\ mV\ s^{-1}$, (B) differential pulse voltammetry (DPV), and (C) an analytic curve obtained through DPV. All measurements were carried out in 1.0 $mol\ L^{-1}$ potassium phosphate buffer (at pH 1.5).

Preliminarily, we proposed applications in electrochemical sensors for detecting Cr(VI), however, the films' properties suggest that these films, chiefly the agar/PANI, have a large potential for application in other types of sensors. We believe that PVS may be satisfactorily replaced both by agar and carrageenan in the study and applicability of self-assembled thin films, as in addition to being polymers obtained from natural sources, they come from renewable source, have low total cost and improve the electrochemical stability of PANI.

4. Conclusions

Polyaniline LbL thin films were prepared together with agar or carrageenan, natural polymers extracted from the cell wall of red seaweeds. The form of preparation of these films has a strong effect upon their final properties. It could be observed that both agar and carrageenan improved the electrochemical stability of PANI, working as a type of antioxidant for the polymer. The results obtained by UV–vis showed that the agar/PANI films exhibit highly regular growth, and the film's thickness can be controlled by the number of bilayers adsorbed. The analyses carried out by AFM showed that the deposition sequence directly influences the morphology and roughness of the films produced. The agar/PANI film was also tested in the electrochemical detection of Cr(VI) and limits of detection of 2.48 $\mu mol\ L^{-1}$ were attained. The present study also demonstrated the advantages of the use of natural polymers for the structuring of thin films, compared to the use of PVS, a polymer that has been widely used in the production of this type of film.

Acknowledgements

This study received financial support from CNPq and Nanobiomed CAPES Network, Brazil. PE is the recipient of a *Ciência Sem Fronteiras* grant from the Brazilian Government. Q7

References

[1] Y. Taga, Mater. Sci. Eng. C 15 (2001) 231–323.
[2] H. Hu, J.M. Saniger, J.G. Bañuelos, Thin Solid Films 347 (1999) 241–247.
[3] A.T. Royappa, M.F. Rubner, Langmuir 8 (1992) 3168–3177.
[4] J.F. Rusling, E.G. Hvastkovs, D.O. Hull, J.B. Schenkman, Chem. Commun. 14 (2008) 141–154.
[5] G. Decher, Science 277 (1997) 1232–1237.
[6] F.N. Crespilho, V. Zucolotto, O.N. Oliveira Jr., F.C. Nart, Int. J. Electrochem. Sci. 1 (2006) 194–214.
[7] M.C. Santos, M.L. Munford, R.F. Bianchi, Mater. Sci. Eng. B 177 (2012) 359–366.
[8] T. Blythe, D. Bloor, Electrical Properties of Polymers, Cambridge University Press, 2002.
[9] F.R.R. Teles, L.P. Fonseca, Mater. Sci. Eng. C 28 (2008) 1530–1543.
[10] A.M. Bonastre, P.N. Bartlett, Anal. Chim. Acta 676 (2010) 1–8.
[11] S. Hanstein, A. Martinez-Bonastre, U. Nestler, P.N. Bartlett, Sens. Actuat. B: Chem. 125 (2007) 284–300.
[12] C. Sanchis, M.A. Ghanem, H.J. Salavagione, E. Morallón, P.N. Bartlett, Bioelectrochemistry 80 (2011) 105–113.
[13] F. Arslan, S. Ustabas, H. Arslan, Sensors 11 (2011) 8152–8163.
[14] P.D. Gaikwad, D.J. Shirale, P.A. Savale, K. Datta, P. Ghosh, A.J. Pathan, G. Rabbani, M.D. Shirsat, Int. J. Electrochem. Sci. 2 (2007) 488–497.
[15] Z.A. Mangombo, D. Key, E.I. Iwuoha, P.G.L. Baker, Insciences J. 3 (2013) 1–23.
[16] Z.A. Mangombo, P. Baker, E. Iwuoha, D. Key, Microchim. Acta 170 (2010) 267–273.
[17] P.M. Ndangili, T.T. Waryo, M. Muchindu, P.G.L. Baker, C.J. Ngila, E.I. Iwuoha, Electrochim. Acta 55 (2010) 4267–4273.
[18] D. Plackett, Biopolymers: New Materials for Sustainable Films and Coatings, Wiley, 2011.
[19] V.K. Thakur, M.K. Thakur, J. Clean Prod. (2014) 1–15.
[20] I.M.S. Araujo, M.F. Zampa, J.B. Moura, J. Borges, J.R. Santos Jr., P. Eaton, V. Zucolotto, L.M.C. Veras, R.C.M. De Paula, J.P.A. Feitosa, J.R.S.A. Leite, C. Eiras, Mater. Sci. Eng. C 32 (2012) 1588–1593.
[21] S.B.A. Barros, C.M.S. Leite, A.C.F. Brito, J.R. Santos Jr., V. Zucolotto, C. Eiras, Int. J. Anal. Chem. (2012) 1–10.
[22] M.F. Zampa, I.M.S. Araujo, V. Costa, C.H. Nery Costa, J.R. Santos Jr., V. Zucolotto, C. Eiras, J.S.A. Leite, Nanomed. Nanotechnol. 5 (2009) 352–358.
[23] M.F. Zampa, A.F. De Brito, I.L. Kitagawa, C.J.L. Constantino, O.N. Oliveira Jr., H.N. Da Cunha, V. Zucolotto, J.R. Dos Santos Jr., C. Eiras, Biomacromolecules 8 (2007) 3408–3413.
[24] S. Sowmya, J.D. Bumgardener, K.P. Chennazhi, S.V. Nair, R. Jayakumar, Prog. Polym. Sci. 38 (2013) 1748–1772.
[25] M.G.A. Vieira, M.A. Silva, L.O. Santos, M.M. Beppu, Eur. Polym. J. 47 (2011) 254–263.
[26] S. Boddohi, M.J. Kipper, Adv. Mater. 22 (2010) 2998–3016.
[27] K.H.M. Cardozo, T. Guaratini, M.P. Barros, V.R. Falcao, A.P. Tonon, N. Lopes, S. Campos, M.A. Torres, A.O. Souza, P. Colepicolo, E. Pinto, Comp. Biochem. Physiol. C 146 (2007) 60–78.
[28] J.S. Maciel, L.S. Chaves, B.W.S. Souza, D.I.A. Teixeira, A.L.P. Freitas, J.P.A. Feitosa, R.C.M. Paula, Carbohydr. Polym. 71 (2008) 559–565.
[29] A. Jensen, Hydrobiologia 260 (1993) 15–23.
[30] D. Mchugh, FAO Fish. Tech. 44 (2003).
[31] M. Ganesan, S. Thiruppathi, B. Jha, Aquaculture 256 (2006) 201–211.
[32] S.R. Cunha, F.D. Pazeto, D.E.V. Crestani, G.B. Lima, J. Nascimento, F. Santanna, G.C. Manzoni, A.W.C. Marenzi, L.L. Mafra Jr., Notas Téc. Facimar (1999) 17–24.
[33] W.G. Charles, S. llan, E.G. Melvyn, Y. Wilfred, Carbohydr. Res. 129 (1984) 189–196.
[34] M. Armana, S.A.U. Qader, Carbohydr. Polym. 88 (2012) 1264–1271.
[35] C.T. Andrade, E.G. Azero, L. Luciano, M.P. Gonçalves, Int. J. Biol. Macromol. 27 (5) (2000) 349–353.
[36] L.H.C. Mattoso, Quim. Nova 19 (1996) 388–399.
[37] W. Kern, Semicond. Int. 7 (1984) 94–98.
[38] P. Eaton, P. West, Atomic Force Microscopy, Oxford University Press, Oxford, UK, 2010.
[39] S. Mazumder, P.K. Ghosal, C.A. Pujol, M.J. Carlucci, E.B. Damonte, B. Ray, Int. J. Biol. Macromol. 31 (2002) 87–95.
[40] M. Sekral, P. Legrand, Spectrochim. Acta 49 (2) (1993) 209–221.
[41] E. Tojo, J. Prado, Carbohydr. Res. 338 (2003) 1309–1312.
[42] C. Eiras, I.N.G. Passos, A.C.F. De Brito, J.R.S. Junior, V. Zucolotto, O.N. Oliveira Jr., I.L. Kitagawa, C.J.L. Constantino, H.N. Cunha, Quim. Nova (2007) 30.
[43] C. Dhand, M. Das, M. Datta, B.D. Malhotra, Biosens. Bioelectron. 26 (2011) 2811–2821.
[44] W.S. Huang, B.D. Humphrey, A.G. Macdiarmid, J. Chem. Soc., Faraday Trans. 1 82 (1986) 2385–2400.
[45] G. Jiao, G. Yu, J. Zhang, H.S. Ewart, Mar. Drugs 9 (2011) 196–223.
[46] H. Qi, Q. Zhang, T. Zhao, R. Chen, H. Zhang, X. Niu, Int. J. Biol. Macromol. 37 (4) (2005) 195–199.
[47] Z. Zhang, Q. Zhang, J. Wang, X. Shi, H. Song, J. Zhang, Carbohydr. Polym. 78 (2009) 449–453.
[48] M.C.H. Souza, C.T. Marques, C.M.G. Dore, F.R.F. Silva, H.A.O. Rocha, E.L. Leite, J. Appl. Phycol. 19 (2007) 153–160.
[49] F.M. Kelly, J.H. Johnston, T. Borrmann, M.J. Richardson, Eur. J. Inorg. Chem. (2007) 5571–5577.
[50] X. Xie, T. Gan, D. Sun, K. Wu, Fuller. Nanotub. Carbon Nanostruct. 16 (2008) 103–113.
[51] S. Pruneanu, E. Veress, I. Marian, L. Oniciu, J. Mater. Sci. 34 (1999) 2733–2739.
[52] A.J. Bard, L.R. Faulkner, Electrochemical Methods Fundamentals and Applications, John Wiley & Sons, New York, 2001.
[53] Y. Fu, R.A. Weiss, Synth. Met. 84 (1997) 103–104.
[54] B. Kavitha, K. Prabakar, K. Siva Kumar, D. Srinivasu, Ch. Srinivas, V.K. Aswal, V. Siriguri, N. Narsimlu, IOSR-JAC 2 (2012) 16–19.
[55] Y. Cao, P. Smith, A.J. Heeger, Synth. Met. 32 (1989) 263–281.
[56] N.V. Bhat, D.T. Seshadri, R.S. Phadke, Synth. Met. 130 (2002) 185–192.
[57] Z. Chenyun, Z. Shengnan, G. Picheng, M. Hongmin, W. Qin, Thin Solid Films 570 (2014) 27–32.
[58] P.A. Patel, J. Jeon, P.T. Mather, A.V. Dobrynin, Langmuir 21 (2005) 6113–6122.
[59] M.R. Samani, S.M. Borghei, A. Olad, M.J. Chaichi, J. Hazard. Mater. 184 (2010) 248–254.
[60] A.M. Khah, R. Ansari, A.F. Delavar, Z. Mosayebzadeh, Bull. Korean Chem. Soc. 33 (4) (2012) 1247–1252.
[61] T.J. O'brien, S. Ceryak, S.R. Patierno, Mutat. Res. 533 (2003) 3–363.
[62] K.K. Krishnani, M. Srinives, B.C. Mohapatra, V.M. Boddu, X. Meng, A. Mulchandani, J. Hazard. Mater. 252–253 (2013) 99–106.
[63] A.G. Yavuz, E. Dincturk-Atalay, A. Uygun, F. Gode, E. Aslan, Desalination 279 (2011) 325–331.
[64] P.A. Kumar, S. Chakraborty, J. Hazard. Mater. 162 (2009) 1086–1098.
[65] M.C. Tsai, P.Y. Chen, Talanta 76 (3) (2008) 9–533.
[66] A. Zazoua, R. Kherrat, M.H. Samar, A. Errachid, N. Jaffrezic-Renault, F. Bessueille, D. Léonard, Mater. Sci. Eng. C 28 (2008) 1014–1019.
[67] S. Banerjee, P. Sarkar, Sens. Lett. 9 (2011) 1370–1375.
[68] A. Safavi, N. Maleki, H.R. Shahbaazi, Talanta 68 (2006) 1113–1119.
[69] E. Song, J.W. Choi, Nanomaterials 3 (3) (2013) 498–523.
[70] L. Pereira, A. Sousa, H. Coelho, A.M. Amado, P.J.A. Ribeiro-Claro, Biomol. Eng. 20 (2013) 223–228.

Please cite this article in press as: E.A. de Oliveira Farias, et al., Mater. Sci. Eng. B (2015), http://dx.doi.org/10.1016/j.mseb.2015.05.004